Int. J. Heat Mass Transfer. Vol. 22, pp. 1125–1135
© Pergamon Press Ltd. 1979. Printed in Great Britain

0017-9310/79/0701-1125 $02.00/0

A THEORETICAL INVESTIGATION OF THE EFFECT OF FREESTREAM TURBULENCE ON SKIN FRICTION AND HEAT TRANSFER FOR A BLUFF BODY

BENGT SUNDÉN
Department of Applied Thermo and Fluid Dynamics, Chalmers University of Technology, Fack, 40220 Göteborg, Sweden

(*Received* 3 *January* 1978 *and in revised form* 6 *February* 1979)

Abstract—A theoretical investigation of the effect of freestream turbulence on skin friction and heat transfer around a circular cylinder in cross flow is presented. The flow field is divided into different regions. A two-equation turbulence model together with proper coordinate transformations is used. The calculations are performed for Reynolds numbers in the range of 12 500–50 000 and turbulence intensities in the range of $Tu_\infty = 1.25$–6.1% and turbulent length scales in the range of $\Lambda_{f\infty}/D = 0.1$–$1.6$. Effect on skin friction and heat transfer of both turbulence intensity and turbulent length scale is found. Good agreement with experiment is achieved.

NOMENCLATURE

a, cylinder radius;
c, coefficient in the boundary layer calculation [1/s];
C_F, skin friction coefficient;
c_1, c_2, c_3, coefficients in the formula for the velocity outside the boundary layer;
D, cylinder diameter;
e, turbulent kinetic energy;
e_∞, value of e far away from the cylinder;
e', dimensionless turbulent kinetic energy in the outer inviscid region;
E, dimensionless turbulent kinetic energy in the boundary layer region;
E_1, value of E on the boundary between the boundary layer region and the outer inviscid region;
exp, exponential function;
$F(\eta)$, pressure function;
Fr_D, Frössling's number $(= Nu_D/\sqrt{Re_D})$;
h, film heat transfer coefficient;
i, imaginary unit;
k_1, constant;
k, thermal conductivity;
Nu_D, Nusselt number based on cylinder diameter $(= hD/k)$;
p, pressure;
p_0, stagnation point pressure;
Pr, Prandtl number;
Pr_T, turbulent Prandtl number;
r, radial co-ordinate;
Re_D, Reynolds number based on cylinder diameter $(= U_\infty D/\nu)$;
R_T, turbulent Reynolds number $(= e/\nu\omega)$;
S_{ij}, mean rate of strain tensor;
t, temperature;
t_w, surface temperature of the cylinder;
t_∞, temperature outside the boundary layer;
T, dimensionless temperature in the boundary layer;
Tu_∞, turbulence intensity far away from the cylinder $(= \sqrt{u'^2}/U_\infty)$;
u_i, velocity vector;
u, velocity in x-direction;
u', dimensionless velocity in the x-direction;
U_∞, mean velocity far away from the cylinder;
U', dimensionless velocity outside the boundary layer;
$U(\eta)$, velocity function in the x-direction for the stagnation region;
$\sqrt{u'^2}$, r.m.s.-value of the velocity fluctuations in the x-direction;
v, velocity in y-direction;
$V(\eta)$, velocity function in y-direction;
$\sqrt{v'^2}$, r.m.s.-value of the velocity fluctuations in the y-direction;
W, dimensionless pseudovorticity in the boundary layer;
W_1, value of W on the boundary between the boundary layer region and the outer inviscid region;
$\sqrt{w'^2}$, r.m.s.-value of the velocity fluctuations in the z-direction;
x, y, z, rectilinear co-ordinate system.

Greek symbols

$\alpha, \alpha^*, \beta, \beta^*, \sigma, \sigma^*$, constants in the turbulence model equations;
δ_{ij}, Kronecker's delta;
ε, turbulent eddy viscosity;
ε', dimensionless turbulent eddy viscosity;
η, co-ordinate in use in the outer inviscid region;
η, dimensionless co-ordinate in use in the boundary layer region;

η_{max}, maximum value of η in the boundary layer;
η', dimensionless co-ordinate in use in the outer inviscid region;
θ, angle in the polar co-ordinate system;
Λ, turbulent length scale;
$\Lambda_{f\infty}$, longitudinal turbulent macro length scale far away from the cylinder;
μ, dynamic viscosity ($= \mu/\rho$);
ξ, co-ordinate in use in the outer inviscid region;
ξ, dimensionless co-ordinate in use in the boundary layer region;
ξ', dimensionless co-ordinate in use in the outer inviscid region;
ρ, density;
σ_{ij}, deviatoric stress tensor;
φ, angle measured from the forward stagnation point;
ψ, stream function;
ω, turbulent pseudovorticity;
ω_∞, value of ω far away from the cylinder;
ω', dimensionless turbulent pseudovorticity in the outer inviscid region.

INTRODUCTION

BY MANY experimental investigations around for instance a circular cylinder in cross flow, it has been shown that the heat transfer coefficient can be much enlarged if turbulence is introduced into the flow field (see Kestin [1].) However, there seems to be some spread in the experimental results. This is mostly because only the effect of the turbulence intensity (Tu_∞) has been studied. Van der Hegge Zijnen [2] made a systematic investigation of the combined effect of the turbulent scale ($\Lambda_{f\infty}$) and the turbulence intensity (Tu_∞) on the mean heat transfer coefficient. His extensive measurements were so arranged that the scale of the turbulence was either very large or comparable with the diameter of the cylinder. He established that the ratio Nu_{turb}/Nu_{lam} systematically increased with turbulence intensity. For a constant turbulence intensity he found that the heat transfer coefficient increased with scale if $0 < \Lambda_{f\infty}/D < 1.6$ and decreased with scale if $\Lambda_{f\infty}/D > 1.6$. Also other workers have tried to study the effect of the turbulent length scale ($\Lambda_{f\infty}$). Appelqvist [3] investigated the effect of turbulence intensity on heat transfer with a turbulent length scale ratio in the very narrow range of $0.04 < \Lambda_{f\infty}/D < 0.18$. No conclusion of the effect of the turbulent length scale could thus be made. Dyban *et al.* [4] investigated both the effect of turbulence intensity and turbulent length scale on heat transfer but found only small effects of the turbulent length scale. Boulos and Pei [5] recently performed measurements in which they varied the turbulent length scale ratio in the range of $0.1 < \Lambda_{f\infty}/D < 0.4$, but they found no systematic influence of the turbulent length scale on heat transfer. Recently, Liljevall [6, 7] made a systematic investigation of the combined effect of the turbulence intensity and the turbulent length scale ($0.1 < \Lambda_{f\infty}/D < 1.5$) on the local and the mean heat transfer coefficient. He found that an increase in both turbulence intensity and turbulent length scale increased the heat transfer coefficient. Some of Liljevall's results are used in this report.

In this work a theoretical investigation of the effect of freestream turbulence on skin friction coefficient C_F and heat transfer coefficient $Fr_D = Nu_D/\sqrt{Re_D}$ is done for a circular cylinder in cross flow. Also the development of the turbulence structure when approaching the cylinder as well as the development of the boundary layer is studied. The investigations are done for different turbulence intensities Tu_∞ and turbulent length scales $\Lambda_{f\infty}$ and different Reynolds numbers Re_D, all in a systematic way.

Of previous theoretical investigations in this field, all except one concerned the stagnation region.

The works by Lighthill [8], Lin [9], and Glauert [10] predicted that freestream oscillations would have little or no effect on mean boundary layer heat transfer or shear stress. This conclusion was confirmed in an analysis by Ishigaki [11, 12], who performed a thorough study of the effect of freestream oscillations of various frequencies on stagnation point flow. Another theoretical study was done by Sutera *et al.* [13]; Sutera [14] and Sadeh *et al.* [15, 16]; who showed that the introduction of vorticity into the freestream resulted in increases in stagnation point heat transfer. They identified the mechanism as stretching of vortex lines in the divergent stagnation point flow.

The first theoretical study which involved a real turbulence parameter was the work by Smith and Kuethe [17]. They used a simple assumption for the turbulent eddy viscosity in the stagnation point boundary layer and achieved good agreement with their own experiment.

Recently Traci and Wilcox [18, 19] presented a study of the effect of freestream turbulence on stagnation point flow and heat transfer using a two-equation turbulence model. They found great effect of the turbulence intensity but only small effect of the turbulent length scale.

The study that will be presented in this report can in some sense be seen as an extension of the study by Traci and Wilcox.

Hunt [20] has formulated a theory based on the rapid distortion theory of Batchelor and Proudman [21] for analysing the distortion of turbulence in a flow sweeping past a bluff body such as a circular cylinder. Studies were only done for an outer inviscid region surrounding the body. No boundary layer calculation and no heat transfer calculation were done.

THE PROBLEM UNDER CONSIDERATION

We are considering a bluff body, in this case a circular cylinder with a diameter D and a constant surface temperature t_w, immersed in a fluid. Far away from the body the flow field is described by

FIG. 1. Problem under consideration.

mean velocity U_∞, freestream turbulence intensity Tu_∞, turbulent length scale $\Lambda_{f\infty}$, and mean temperature t_∞. Reynolds number is greater than 10^4 (see Fig. 1). We now wonder how the skin friction coefficient C_F and the heat transfer coefficient $Fr_D = Nu_D/\sqrt{Re_D}$ are changed by Tu_∞ and $\Lambda_{f\infty}$ and Re_D. Furthermore, we wish to study the development of the turbulence structure.

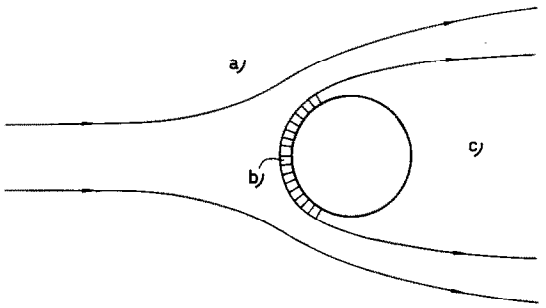

FIG. 2. Model of the flow field.

Model of the flow field

The flow field is divided into three parts (see Fig. 2):

(a) An outer inviscid region;

(b) A boundary layer on the forward side of the cylinder;

(c) A wake region on the backward side of the cylinder.

Hypotheses:

(1) In the outer inviscid region, the freestream turbulence does not disturb the mean flow field;

(2) The flow field is generally assumed to be steady and incompressible.

That hypothesis 1 is a good approximation can be seen from measurements by Liljevall [6] and Britter [22].

We are especially interested in the development of the turbulence structure in the outer inviscid region and the influence of the freestream turbulence on the transport processes within the boundary layer. Since the flow field in the absence of freestream turbulence can not be analysed exactly, it can not be expected that exact results will be obtained for a turbulent flow field. To make the problem mathematically tractable we then use a further hypothesis;

(3) As a first approximation, the effect of the wake region is disregarded.

This hypothesis implies that the outer inviscid mean flow field is equal to the potential flow around the cylinder.

In agreement with the hypotheses the problem is reduced as follows:

(1) Calculation of the development of the turbulence structure when approaching the body in a known outer inviscid mean flow field. The basic purpose of this calculation is to obtain boundary values of the turbulence properties on the boundary between the outer inviscid region and the boundary layer region.

(2) Boundary layer calculation on the forward side of the cylinder.

DESCRIPTION OF THE TURBULENCE STRUCTURE

To describe the turbulence structure, one has to use some turbulence model. We have here chosen the Saffman model. It is a two-equation model and works with the turbulence parameters:

e, turbulent kinetic energy;
ω, turbulent pseudovorticity.

The model was proposed by Saffman [23] and has been used and developed by Wilcox and Alber [24] and Saffman and Wilcox [25]. Traci and Wilcox also used it in their study concerning only the stagnation region. The Saffman model equations for the steady incompressible case are:

Equation for the mean motion:

$$u_j \frac{\partial u_i}{\partial x_j} = -\frac{1}{\rho}\frac{\partial p}{\partial x_i} + \frac{\partial}{\partial x_j}\sigma_{ij}; \tag{1}$$

Mass-conservation equation:

$$\frac{\partial u_i}{\partial x_i} = 0, \tag{2}$$

with

$$\sigma_{ij} = 2(\nu+\varepsilon)S_{ij} - \tfrac{2}{3}e\delta_{ij} \tag{3}$$

$$S_{ij} = (u_{i,j}+u_{j,i})/2; \tag{4}$$

Equation for the turbulent kinetic energy:

$$u_j \frac{\partial e}{\partial x_j} = \alpha^* e(2S_{ij}S_{ij})^{1/2} - \beta^* e\omega + \frac{\partial}{\partial x_j}(\nu+\sigma^*\varepsilon)\frac{\partial e}{\partial x_j}; \tag{5}$$

Equation for the turbulent pseudovorticity:

$$u_j \frac{\partial \omega^2}{\partial x_j} = \alpha\omega^2\left(\frac{\partial u_i}{\partial x_j}\frac{\partial u_i}{\partial x_j}\right)^{1/2} - \beta\omega^3 + \frac{\partial}{\partial x_j}(\nu+\sigma\varepsilon)\frac{\partial \omega^2}{\partial x_j}, \tag{6}$$

with the eddy viscosity as:

$$\varepsilon = e/\omega, \tag{7}$$

and a turbulent length scale:

$$\Lambda = e^{1/2}/\omega; \tag{8}$$

Equation for the temperature field:

$$u_j \frac{\partial t}{\partial x_j} = \frac{\partial}{\partial x_j}\left(\frac{\nu}{Pr} + \frac{\varepsilon}{Pr_T}\right)\frac{\partial t}{\partial x_j}. \tag{9}$$

The numerical values of the constants are:

$$\alpha^* = 0.3, \quad \alpha = 0.2638, \quad \beta = 0.18,$$
$$\beta^* = 0.09, \quad \sigma = \sigma^* = 0.5.$$

The model equations have been changed by Saffman [26] so that e is taken more directly as the turbulent kinetic energy. In this work the original equations [(1)–(9) above] are used, and e is taken as the turbulent kinetic energy. The turbulent length scale defined by equation (8) is taken as the longitudinal macroscale.

Equations (1)–(9) are now to be used for the two cases mentioned above.

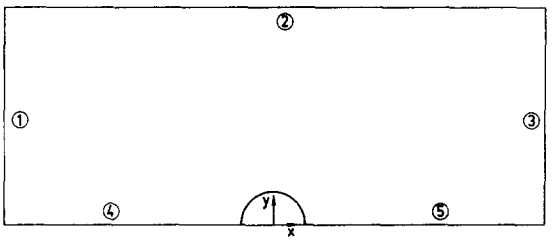

FIG. 3. The original calculation domain (not to scale).

CALCULATION OF THE DEVELOPMENT OF THE TURBULENCE STRUCTURE IN THE OUTER INVISCID REGION

The calculation domain is shown in Fig. 3. The flow field is assumed to be symmetric around the stagnation lines. The equations to be solved are:

$$u\frac{\partial e}{\partial x} + v\frac{\partial e}{\partial y} = \alpha^* e\left(2\left(\frac{\partial u}{\partial x}\right)^2 + \left(\frac{\partial u}{\partial y}\right)^2 + 2\frac{\partial u}{\partial y}\frac{\partial v}{\partial x} + \left(\frac{\partial v}{\partial x}\right)^2 + 2\left(\frac{\partial v}{\partial y}\right)^2\right)^{1/2} - \beta^* e\omega + \frac{\partial}{\partial x}\left(\sigma^*\varepsilon\frac{\partial e}{\partial x}\right) + \frac{\partial}{\partial y}\left(\sigma^*\varepsilon\frac{\partial e}{\partial y}\right) \tag{10}$$

$$u\frac{\partial \omega^2}{\partial x} + v\frac{\partial \omega^2}{\partial y} = \alpha\omega^2\left(\left(\frac{\partial u}{\partial x}\right)^2 + \left(\frac{\partial u}{\partial y}\right)^2 + \left(\frac{\partial v}{\partial x}\right)^2 + \left(\frac{\partial v}{\partial y}\right)^2\right)^{1/2} - \beta\omega^3 + \frac{\partial}{\partial x}\left(\sigma\varepsilon\frac{\partial \omega^2}{\partial x}\right) + \frac{\partial}{\partial y}\left(\sigma\varepsilon\frac{\partial \omega^2}{\partial y}\right). \tag{11}$$

The boundary conditions are:

Boundary 1: The turbulence is assumed to be isotropic and homogeneous. We have

$$e_\infty = (\overline{u'^2} + \overline{v'^2} + \overline{w'^2})/2 \text{ and } Tu_\infty = \frac{\sqrt{u'^2}}{U_\infty};$$

isotropy gives

$$e_\infty = \tfrac{3}{2}U_\infty^2 Tu_\infty^2 \tag{12}$$

$$\omega_\infty = \frac{e_\infty^{1/2}}{\Lambda_{f\infty}}. \tag{13}$$

Boundary 2: This boundary is assumed to be so far away from the body that the theory of decaying turbulence is valid.

Boundary 3: Also this boundary is assumed to be so far away from the body that the disturbances from the body can be neglected and the turbulence begins to decay.

Boundary 4 and 5: The symmetry requires the conditions

$$\partial e/\partial y = 0 \tag{14}$$

$$\partial \omega^2/\partial y = 0. \tag{15}$$

Finally, we have the boundary conditions between the outer inviscid region and the boundary layer region. Here we use:

$$\partial e/\partial r = 0 \tag{16}$$

$$\left(\frac{\partial \omega^2}{\partial r}\right)_{\substack{\text{outer inviscid}\\ \text{region}}} = \left(\frac{\partial \omega^2}{\partial r}\right)_{\substack{\text{boundary layer}\\ \text{region}}} \tag{17}$$

$$\omega^2_{\substack{\text{outer inviscid}\\ \text{region}}} = \omega^2_{\substack{\text{boundary layer}\\ \text{region.}}} \tag{18}$$

Condition (16) is based on the following assumption.

Since the velocity gradients of the mean flow field are large even outside the boundary layer, the turbulent kinetic energy will be amplified in the outer inviscid region. The molecular viscosity is assumed to be of importance in the whole boundary layer. Since the turbulent kinetic energy must be zero at the body surface, the turbulent energy must be broken down within the boundary layer. (That is, viscous dissipation is assumed to be the dominating process within the boundary layer.) Thus we must have the condition (16) at the boundary between the outer inviscid region and the boundary layer region. Conditions (17) and (18) are based on the fact that the turbulent pseudovorticity becomes infinite at a smooth solid surface.

Traci and Wilcox, who studied the stagnation region, obtained the corresponding boundary values on the boundary layer edge in the following way. Far away from the body the turbulent energy and the turbulent pseudovorticity were prescribed and conditions on the gradients, which arose from neglecting diffusion far away from the body, were used. This is an initial value problem, which unfortunately is numerically unstable. Instead they had to use a shooting method. Values of the turbulent energy and the turbulent pseudovorticity on the boundary layer edge were guessed. Then the equations were solved iteratively until the conditions far away from the body were satisfied within some per cent.

In this work, the conditions at the boundary layer edge have been based on a physical consideration of the coupling between the outer inviscid region and the boundary layer region. This seems to be very important for a physically correct description of the turbulent length scale.

For accuracy in the numerical treatment we

introduce new rectangular coordinates (ξ, η) by the conformal transformation

$$\xi + i\eta = \frac{1}{\pi}\ln(x+iy) = \frac{1}{\pi}\ln(r\exp(i\theta)). \quad (19)$$

The transformation is shown in Fig. 4. Since this transformation maps a circle area into a rectangular area, the boundary conditions of boundaries 1, 2 and 3 in the original calculation domain (Fig. 3) must be recalculated to be valid for the outer circle line in Fig. 4.

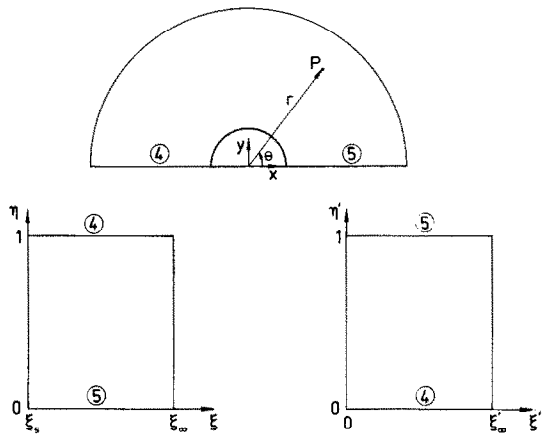

FIG. 4. Picture of the coordinate transformation (not to scale).

From equation (19) we have:

$$\xi = \frac{1}{\pi}\ln r \quad (20)$$

$$\eta = \theta/\pi. \quad (21)$$

For practical reasons we further introduce:

$$\xi' = \frac{1}{\pi}\ln\frac{r}{a} \quad (22)$$

$$\eta' = 1-\theta/\pi. \quad (23)$$

For the mean velocity field, we introduce the stream function ψ. The expression for ψ is here:

$$\psi = U_\infty a\sin(\pi\eta')\{\exp(\pi\xi')-\exp(-\pi\xi')\}. \quad (24)$$

With the transformations (22) and (23), and equation (24) and the following nondimensional variables

$$e' = e/U_\infty^2 \quad (25)$$

$$\omega' = \frac{\omega}{U_\infty}a. \quad (26)$$

Equations (10) and (11) become:

$$\pi\sin(\pi\eta')\{\exp(\pi\xi')+\exp(-\pi\xi')\}\frac{\partial e'}{\partial\eta'} - \pi\cos(\pi\eta')\{\exp(\pi\xi')-\exp(-\pi\xi')\}\frac{\partial e'}{\partial\xi'} = 4\pi^2 e'\alpha^*\exp(-\pi\xi') - \pi^2\beta^* e'\omega'\exp(2\pi\xi') + \frac{\partial}{\partial\xi'}\left(\sigma^*\varepsilon'\frac{\partial e'}{\partial\xi'}\right) + \frac{\partial}{\partial\eta'}\left(\sigma^*\varepsilon'\frac{\partial e'}{\partial\eta'}\right) \quad (27)$$

$$\pi\sin(\pi\eta')\{\exp(\pi\xi')+\exp(-\pi\xi')\}\frac{\partial\omega'^2}{\partial\eta'} - \pi\cos(\pi\eta')\{\exp(\pi\xi')-\exp(-\pi\xi')\}\frac{\partial\omega'^2}{\partial\xi'} = \pi^2\omega'^2\{\alpha 2\sqrt{2}\exp(-3\pi\xi')-\beta\omega'\}\exp(2\pi\xi') + \frac{\partial}{\partial\xi'}\left(\sigma\varepsilon'\frac{\partial\omega'^2}{\partial\xi'}\right) + \frac{\partial}{\partial\eta'}\left(\sigma\varepsilon'\frac{\partial\omega'^2}{\partial\eta'}\right). \quad (28)$$

Equations (27) and (28) are solved numerically by a finite difference technique. The outer circle line (see Figs. 4) is placed at $r/a = 14$ since the corresponding experiment [6] uses $r/a = 14$ as the point far away from the body where the turbulence intensity Tu_∞ and the turbulent length scale $\Lambda_{f\infty}$ are defined.

Since the effect of the wake region is disregarded, the boundary condition between the boundary layer region and the outer inviscid region is used around the whole cylinder surface.

BOUNDARY LAYER CALCULATION

The boundary layer region is divided into two parts:

(a) stagnation region;
(b) region further along the body surface.

For the stagnation region we assume a generalized Hiemenz-flow shown in Fig. 5. We use the coordinate transformations:

$$\xi = \sqrt{c/\nu}\,x \quad (29)$$

$$\eta = \sqrt{c/\nu}\,y, \quad (30)$$

where $c = 4U_\infty/D$ for the cylinder case.

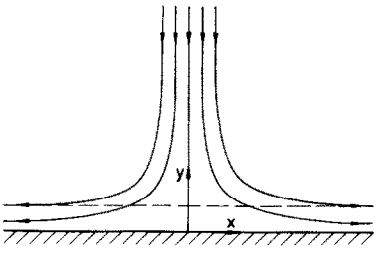

FIG. 5. Generalized Hiemenz-flow in the stagnation region.

The following assumptions are made:

$$u = U(\eta)cx \quad (31)$$

$$v = \sqrt{\nu c}\,V(\eta) \quad (32)$$

$$t = t_w + (t_\infty - t_w)T(\eta) \quad (33)$$

$$p_0 - p = \rho\nu c(F(\eta)+\tfrac{1}{2}\xi^2) \quad (34)$$

$$e = \nu c E(\eta) \quad (35)$$

$$\omega = cW(\eta). \quad (36)$$

The equations for the stagnation boundary layer region now become:

$$\frac{dV}{d\eta} + U = 0 \quad (37)$$

$$V\frac{dU}{d\eta} = 1 - U^2 + \frac{d}{d\eta}\left(1+\frac{E}{W}\right)\frac{dU}{d\eta} \quad (38)$$

$$\frac{d(VE)}{d\eta} = (2\alpha^*|U| - U)E - \beta^* EW + \frac{d}{d\eta}\left(1+\sigma^*\frac{E}{W}\right)\frac{dE}{d\eta} \quad (39)$$

$$\frac{d(VW^2)}{d\eta} = (\sqrt{2}\alpha|U| - U)W^2 - \beta W^3 + \frac{d}{d\eta}\left(1+\sigma\frac{E}{W}\right)\frac{dW^2}{d\eta} \quad (40)$$

$$\frac{d(VT)}{d\eta} = -UT + \frac{d}{d\eta}\left(\frac{1}{Pr}+\frac{E/W}{Pr_T}\right)\frac{dT}{d\eta} \quad (41)$$

plus an equation for $F(\eta)$ not given here.

The boundary conditions are:

$$\eta = 0: \quad U = V = E = T = F = 0$$

$$\eta^2 W = \frac{20}{\beta} \quad (42)$$

$$\eta \to \infty: \quad U \to 1,\ T \to 1,\ E \to E_1,\ W^2 \to W_1^2$$

$$\left(\frac{dW^2}{d\eta}\right)_{\substack{\text{boundary layer}\\ \text{region}}} = \left(\frac{dW^2}{d\eta}\right)_{\substack{\text{outer inviscid}\\ \text{region.}}} \quad (43)$$

Here E_1 and W_1 denote the value of E and W, respectively on the boundary between the boundary layer region and the outer inviscid region. Of course $\eta \to \infty$ must be approximated by some large value $\eta = \eta_{max}$. The value of η_{max} is determined in such a way that the skin friction coefficient C_F and the heat transfer coefficient $Fr_D = Nu_D/\sqrt{Re_D}$ become unique, that is independent of η_{max}. As a consequence, η_{max} is a function of Tu_∞ and $\Lambda_{f\infty}$.

For the calculation further along the surface we use the following transformations:

$$u' = u/U_\infty, \quad v' = v/U_\infty, \quad \xi = \sqrt{c/\nu}\,x,$$
$$\eta = \sqrt{c/\nu}\,y, \quad e = vcE(\xi,\eta), \quad \omega = cW(\xi,\eta), \quad (44)$$
$$t = t_w + (t_\infty - t_w)T(\xi,\eta).$$

The coordinate system is the same as for the stagnation point boundary layer. With the transformations (44) the boundary layer equations become:

$$\frac{\partial u'}{\partial \xi} + \frac{\partial v'}{\partial \eta} = 0 \quad (45)$$

$$u'\frac{\partial u'}{\partial \xi} + v'\frac{\partial u'}{\partial \eta} = U'\frac{dU'}{d\xi} + \frac{2}{\sqrt{Re_D}}\frac{\partial}{\partial \eta}(1+E/W)\frac{\partial u'}{\partial \eta} \quad (46)$$

$$\frac{\partial}{\partial \xi}(u'E) + \frac{\partial}{\partial \eta}(v'E) = \alpha^* E\left(4\left(\frac{\partial u'}{\partial \xi}\right)^2 + \left(\frac{\partial u'}{\partial \eta}\right)^2\right)^{1/2} - \frac{2}{\sqrt{Re_D}}\beta^* EW + \frac{2}{\sqrt{Re_D}}\frac{\partial}{\partial \eta}\left(1+\sigma^*\frac{E}{W}\right)\frac{\partial E}{\partial \eta} \quad (47)$$

$$\frac{\partial}{\partial \xi}(u'W^2) + \frac{\partial}{\partial \eta}(v'W^2) = \alpha W^2\left(2\left(\frac{\partial u'}{\partial \xi}\right)^2 + \left(\frac{\partial u'}{\partial \eta}\right)^2\right)^{1/2} - \frac{2}{\sqrt{Re_D}}\beta W^3 + \frac{2}{\sqrt{Re_D}}\frac{\partial}{\partial \eta}\left(1+\sigma\frac{E}{W}\right)\frac{\partial W^2}{\partial \eta} \quad (48)$$

$$\frac{\partial}{\partial \xi}(u'T) + \frac{\partial}{\partial \eta}(v'T) = \frac{2}{\sqrt{Re_D}}\frac{\partial}{\partial \eta}\left(\frac{1}{Pr}+\frac{E/W}{Pr_T}\right)\frac{\partial T}{\partial \eta}. \quad (49)$$

The boundary conditions of equations (45)–(49) are:

$$\xi = 0: \ u' = 0,\ v' = \frac{\sqrt{vc}}{U_\infty}V(\eta)$$
$$E(0,\eta) = E(\eta)$$
$$W(0,\eta) = W(\eta) \quad (50)$$
$$T(0,\eta) = T(\eta)$$

$$\eta = 0: \ u' = v' = E = T = 0$$

$$\eta^2 W = \frac{20}{\beta} \quad (51)$$

$$\eta \to \infty: \ u' \to U',\ E \to E_1,\ W^2 \to W_1^2,\ T \to 1$$

$$\left(\frac{\partial W^2}{\partial \eta}\right)_{\substack{\text{boundary layer}\\ \text{region}}} = \left(\frac{\partial W^2}{\partial \eta}\right)_{\substack{\text{outer inviscid}\\ \text{region.}}} \quad (52)$$

Again $\eta \to \infty$ must be approximated by $\eta = \eta_{max}$, and this is done in the same way as for the stagnation point boundary layer region. The velocity distribution U' outside the boundary layer is written in the form:

$$U'(\xi) = \sqrt{v/c}(c_1\xi + c_2\xi^3 + c_3\xi^5). \quad (53)$$

For the inviscid flow solution, $c_1 = 4.0$, $c_2 = -2.667$ and $c_3 = 0.533$. However, generally these coefficients must be determined from measurements of the pressure distribution around the cylinder surface.

For the skin friction coefficient C_F we have the following formula:

$$C_F = \frac{4}{\sqrt{Re_D}}\left(\frac{\partial u'}{\partial \eta}\right)_w. \quad (54)$$

For the heat transfer coefficient we have:

$$Fr_D = \frac{Nu_D}{\sqrt{Re_D}} = 2\left(\frac{\partial T}{\partial \eta}\right)_w. \quad (55)$$

In the equations for the temperature field (41) and (49) the Prandtl number is $Pr = 0.7$ and the turbulent Prandtl number is $Pr_T = 0.89$. A turbulent Prandtl number of 0.89 is used, as it is the most appropriate value for boundary layer flows. Equations (37)–(41) and (45)–(49) are solved numerically by a finite difference technique with respect to the boundary conditions (42)–(43) and (50)–(52) respectively.

Numerical solution procedure

All equations are solved by a finite difference technique. The full numerical details will be given in a separate report and here only some principles and

some problems will be mentioned. The first basic idea is that the numerical method should be free of adjustable parameters and also should be as unique as possible.

Equations (27) and (28) are elliptic and since the Reynolds number is very high, upwind differences must be used in the convection terms; otherwise the solution is numerically unstable. In this work a first-order scheme is used for the upwind differences.

Another problem is the matching condition for the turbulent pseudovorticity given in equations (17), (18), (43) and (52). It is very important to have this condition satisfied (at least approximately), especially for the reason of having a physically correct description of the turbulent length scale. Much work has been spent on this matching condition.

Since the equations (27) and (28) are nonlinear and coupled, one has to use some iterative procedure. To speed up convergence, one has to pay special attention to the initial values, and relaxation parameters have to be used.

For the stagnation region the equations are the same as those used by Traci and Wilcox [18, 19], except the form of (38), but the boundary conditions and the solution method are different. Again the equations here ((37)–(41)) are coupled and nonlinear, except (41), and must be solved iteratively. All derivatives can be approximated by second-order differences. Relaxation parameters are used for speeding up convergence.

For the boundary layer calculation further along the surface, the equations are parabolic and the difference scheme is second-order in both the η- and the ξ-direction. The solution procedure is similar to the procedure for the stagnation point boundary layer. The solution method is strongly implicit. For the calculation of the skin friction coefficient C_F and the heat transfer coefficient $Fr_D = Nu_D/\sqrt{Re_D}$ also second-order formulas are used.

In the boundary layer calculations the assumption of α, α^*, β, β^*, σ, σ^* as constants leads to inaccuracy and to disagreement with experimental measurements. For low turbulent Reynolds number $R_T = e/\nu\omega = E/W$ (which is the case in this study), these constants ought to be dependent on R_T. Extensive investigations have shown that the results are very sensitive to the values of α and α^* but rather insensitive to the values of the other constants. For the Saffman-model Wilcox [27] has given a relation $\alpha = f(R_T)$ (the ratio α/α^* was assumed to be the same as for a fully developed turbulent flow) in a study concerning transition processes. For other turbulence models also functional relations of the dependence of similar 'constants' on R_T have been given [28].

Here the functional dependence on R_T has been taken from [28] and the following formulas are used:

$$\alpha^{*\prime} = \alpha^*(R_T = \infty)\, e^{-2.5/(1+R_T/50)} \qquad (56)$$

$$\alpha' = \alpha(R_T = \infty)\, e^{-2.5/(1+R_T/50)}, \qquad (57)$$

where $\alpha^{*\prime}$ is to be used in equations (39) and (47), and α' is to be used in equations (40) and (48).

In this work, the turbulent Reynolds number in the boundary layer is very low and hence the values of $\alpha^{*\prime}$ and α' become very small compared with the corresponding values for a fully developed turbulent flow.

RESULTS AND DISCUSSION

In Fig. 6 is the distribution of the turbulent length scale along the stagnation line shown for the case $Tu_\infty = 6.13\%$ and $Re_D = 25\,900$ for different values of $\Lambda_{f\infty}$. Some corresponding experimental results obtained by Liljevall [6] are given. The agreement between theory and experiment is good. Note however, that the experimental values are for $Re_D = 25\,000$, that the turbulence intensity is 6.20%, and that the scales are not exactly the same far away from the cylinder. In Fig. 7 is the distribution of the turbulent energy along the stagnation line shown for the case $Re_D = 25\,900$, $Tu_\infty = 6.13\%$ and $\Lambda_{f\infty}$

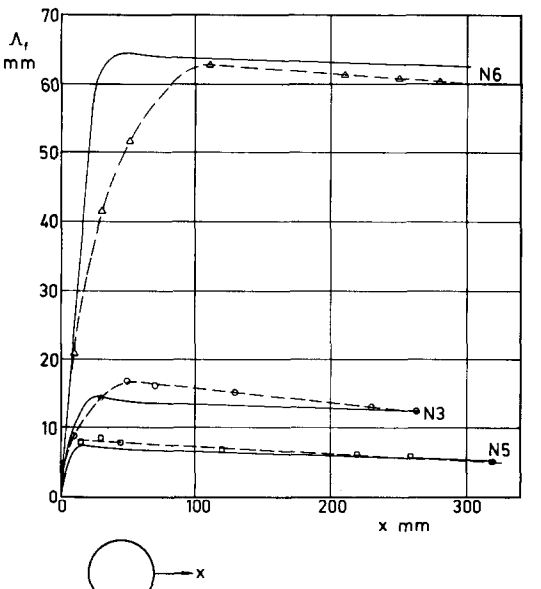

FIG. 6. Distribution of turbulent length scale along the stagnation line for $Tu_\infty = 6.13\%$ and $Re_D = 25\,900$. Dashed lines: experimental values from Liljevall [6] for $Tu_\infty = 6.20\%$ and $Re_D = 25\,000$.

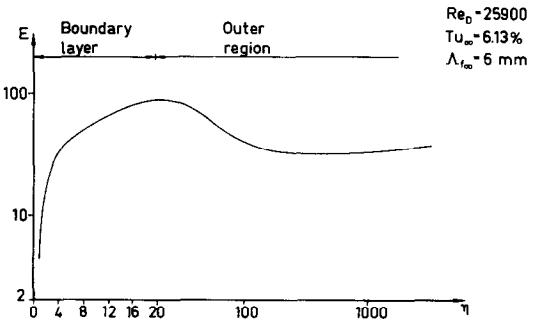

FIG. 7. Distribution of turbulent energy along the stagnation line.

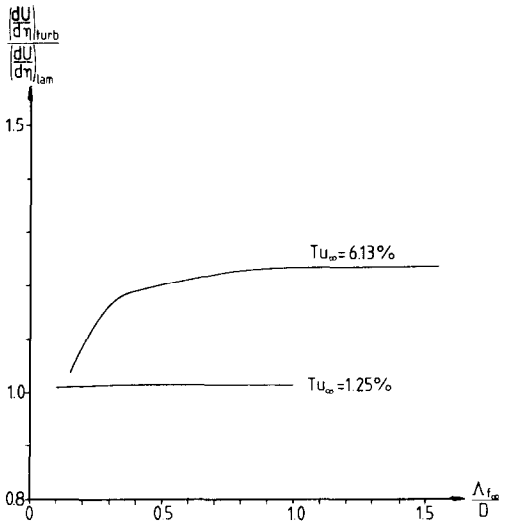

FIG. 8. "Skin friction" ratio in the stagnation region.

$= 6$ mm. ($\Lambda_{f\infty}/D = 0.146$.) No experimental values are available for comparison, but the amplification of turbulent energy due to vortex stretching is evident. The results are in good agreement with the calculations done by Traci and Wilcox [18, 19] and with measurements performed by Bearman [29]. The vortex stretching is in this calculation modeled by the production terms in the equations for e and ω^2.

In Fig. 8 the gradient of the velocity function ($U(\eta)$) at the wall compared with the corresponding laminar gradient is shown for constant values of the turbulence intensity as a function of the ratio turbulent length scale to cylinder diameter $\Lambda_{f\infty}/D$. The Reynolds number is $Re_D = 25\,900$.

The heat transfer coefficient $Fr_D = Nu_D/\sqrt{Re_D}$ is shown as a function of $\Lambda_{f\infty}/D$ for constant turbulence intensities in Fig. 9. The results are given for the stagnation region.

From the results in Figs. 8 and 9 we may conclude that the appearance of turbulent motion in the

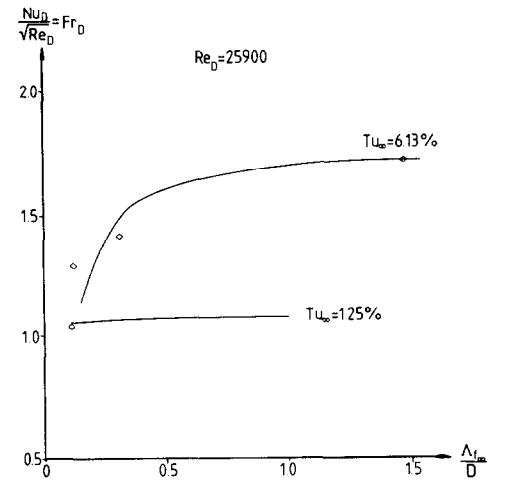

FIG. 9. Heat transfer coefficient in the stagnation region. Experimental values from Liljevall [6]: $Tu_\infty = 6.20\%$ and $Re_D = 25\,000$; $Tu_\infty = 1.25\%$ and $Re_D = 25\,900$.

freestream causes disturbances in the laminar boundary layer and that these disturbances affect the transport processes through the boundary layer.

From equations (12) and (13), we find the following expression for the ratio of imposed turbulent eddy viscosity to molecular viscosity:

$$\frac{\varepsilon_\infty}{\nu} = \sqrt{3/2}\, Re_D Tu_\infty \Lambda_{f\infty}/D. \tag{58}$$

From this equation we may assume that Reynolds number, turbulence intensity and the ratio of turbulent length scale to cylinder diameter influence the momentum transfer (and thereby the skin friction coefficient) and the heat transfer rate. (In this study we have $19.1 < \varepsilon_\infty/\nu < 5780$. The ratio ε/ν undergoes, of course, alterations when the fluid approaches the cylinder. This is evident from Figs. 6 and 7.) Figures 8 and 9 show that for $Tu_\infty = 6.13\%$ the influence of $\Lambda_{f\infty}/D$ on the "skin friction" ratio and the heat transfer coefficient is large but for $Tu_\infty = 1.25\%$ the effect of $\Lambda_{f\infty}/D$ is only very slight.

At this point it may be interesting to note that van der Hegge Zijnen [2] found an optimum value of the ratio $\Lambda_{f\infty}/D$ for which the mean heat transfer coefficient for a given turbulence intensity and Reynolds number was a maximum. The optimum value of $\Lambda_{f\infty}/D$ was about 1.6. In this study only values of $\Lambda_{f\infty}/D$ up to 1.54 have been investigated. Another interesting point of comparison is the fact that van der Hegge Zijnen found the increase of the mean heat transfer coefficient with $\Lambda_{f\infty}/D$ (for $0 < \Lambda_{f\infty}/D < 1.6$) to be greater at higher turbulence intensities and higher Reynolds numbers, exactly as obtained in this work. In Fig. 9 also some experimental values of $Fr_D = Nu_D/\sqrt{Re_D}$ from Liljevall [6] have been given. However, his experiments were done with a Gardon-probe (see [3] and [6]) and this gives the heat transfer coefficient as $k_1 Nu_D/\sqrt{Re_D}$, where k_1 is a constant. k_1 was not evaluated in the experiments. Here k_1 has been determined in such a way that the calculated and measured values overlapped in one point. (Experimental value for $Tu_\infty = 6.2\%$, $\Lambda_{f\infty}/D = 1.47$ and $Re_D = 25\,000$ was set equal to theoretical value for $Tu_\infty = 6.13\%$, $\Lambda_{f\infty}/D = 1.54$ and $Re_D = 25\,900$.)

Similar results to those given in Figs. 8 and 9 were presented by Traci and Wilcox [18, 19]. However, they found only a slight effect of the turbulent length scale on the heat transfer coefficient and considered only small length scale ratios.

The effect of freestream turbulence on the skin friction coefficient along the cylinder surface is shown in Fig. 10 for $Re_D = 25\,900$. The ratio $(C_F)_{turb}/(C_F)_{lam}$ is almost constant over 40 degrees away from the stagnation point for a given turbulence intensity and a given ratio of turbulent length scale to cylinder diameter. In Figs. 11 and 12, the effect of freestream turbulence on the heat transfer coefficient along the cylinder surface is shown. Experimental values from Liljevall [6] are inserted. The difference between the

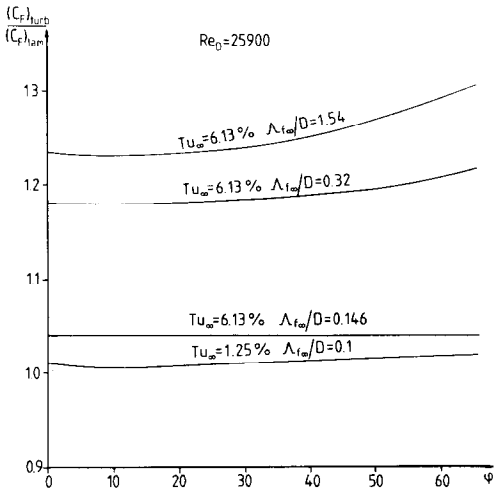

FIG. 10. Ratio between skin friction coefficients along the cylinder surface.

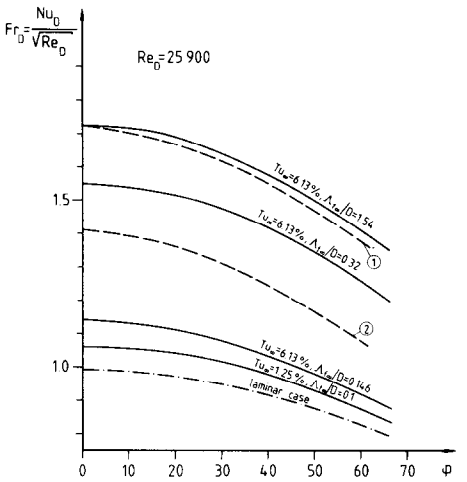

FIG. 11. Heat transfer coefficient along the cylinder surface. Dashed lines: Experiment from Liljevall [6]: ① $Re_D = 25000$, $Tu_\infty = 6.20\%$, $\Lambda_{f\infty}/D = 1.47$; ② $Re_D = 25000$, $Tu_\infty = 6.20\%$, $\Lambda_{f\infty}/D = 0.31$.

calculated curve, $Tu_\infty = 6.13\%$; $\Lambda_{f\infty}/D = 1.54$; $Re_D = 25900$, and the experimental curve marked with a ① in Fig. 11 is at most 2%.

For the experimental curve marked with a ② (Fig. 11) the difference between the corresponding theoretical curve is 8% at the stagnation point and 15% away from the stagnation point.

In Fig. 11 also the heat transfer coefficient for the laminar case is given. We see that the appearance of turbulence in the freestream greatly affect the heat transfer coefficient. (Both turbulence intensity and turbulent length scale influence the heat transfer.)

For the case $Tu_\infty = 6.13\%$, $\Lambda_{f\infty}/D = 0.32$ and $Re_D = 12500$ shown in Fig. 12, we have 8% difference between calculated and measured curves at the stagnation point and 14% at 60° away from the stagnation point. We also have a difference in the slope of the curves. For the case $Tu_\infty = 1.25\%$, $\Lambda_{f\infty}/D = 0.11$ and $Re_D = 50000$, shown in Fig. 12,

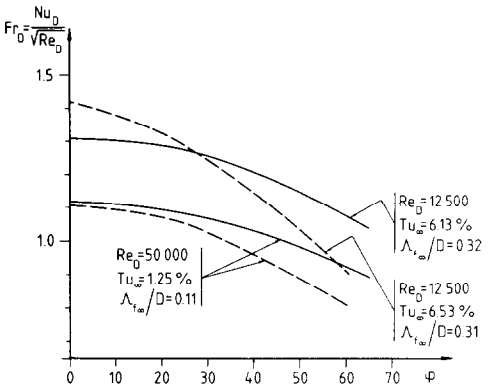

FIG. 12. Heat transfer coefficient along the cylinder surface. —— Theory. – – – Experiment from Liljevall [6].

the difference between the calculated and the experimental curve is lower than 5% between $0° < \varphi < 40°$. At 60°, the difference is 10%.

The difference in slope between calculated and experimental curves, especially in Fig. 12, is due to differences in the velocity distribution outside the boundary layer. In the calculations, potential flow was assumed. In the experiments by Liljevall no measurement of the pressure distribution around the cylinder surface was performed. Thus the coefficients c_1, c_2 and c_3 in equation (53) could not be determined. With experimental values of c_1, c_2 and c_3 (available in the literature) much better agreement between theory and experiment is achieved (for the cases in Fig. 12, within 5%).

The enhancement effect of the freestream turbulence on the local skin friction coefficient and the heat transfer coefficient over the whole boundary layer region is probably the result of boundary layer penetration by the disturbances caused by the freestream turbulence. The distortion of the mean flow field both outside and inside the boundary layer also plays an important role because of the gradients of the mean flow field greatly affect the distributions of the turbulent kinetic energy and the turbulent vorticity.

A study of the calculated velocity and temperature profiles along the cylinder surface shows that the boundary layer can not be said to be a fully turbulent boundary layer but rather a more or less disturbed laminar boundary layer.

The displacement thickness and the momentum thickness of the boundary layer have been found to increase with turbulence intensity but to remain rather unaffected by the turbulent length scale.

From the results presented here, we see that the effect of freestream turbulence on the skin friction coefficient is smaller than the effect on the heat transfer coefficient. This is in agreement with the stagnation point analysis of Smith and Kuethe [17] and the vorticity amplification model of Sutera [14] (for the stagnation region) and the stagnation point calculations by Traci and Wilcox [18, 19]. The effect of Reynolds number (or more strictly $Tu_\infty \sqrt{Re_D}$) on the heat transfer coefficient can be studied in Fig. 13.

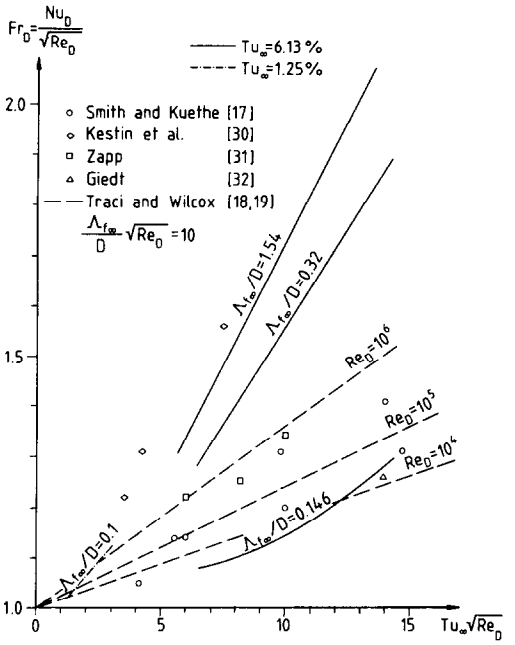

FIG. 13. Reynolds number effect on the heat transfer coefficient in the stagnation region.

The results are only given for the stagnation region but the principal results are the same for the whole boundary layer. In Fig. 13 also some of the oldest experimental data in this field are given. The comparison with these data is difficult to make since mostly only the Reynolds number and the turbulence intensity are given. However, the experimental data are found to fall in between the calculated curves. In Fig. 13 the results obtained by Traci and Wilcox have also been incorporated. Their results are for a constant length scale ratio $\Lambda_{f\infty}/D\sqrt{Re_D} = 10$ and for a different Reynolds number. Although the results calculated by Traci and Wilcox are presented in another way, one can see that the results calculated in this work indicate a greater effect of the freestream turbulence (especially of the turbulent length scale) on the heat transfer coefficient.

The laminar results used in this work are obtained as the special case when freestream turbulence is not present. Of course, the well-known series solutions by Blasius [33] and Frössling [34] could be used, but there is no significant difference between the series solutions and the special case mentioned above.

CONCLUSION

A theoretical investigation of the effect of freestream turbulence on skin friction and heat transfer has been presented. Effect of both turbulence intensity and turbulent length scale has been found. Great simplifications have been used. Nevertheless, decent agreement with corresponding experiment has been found.

The most critical simplification is the neglect of the wake region (hypothesis 3). It is probably worth abandoning this simplification (although very difficult) and using a wake model to obtain a better description of the mean flow field around the cylinder.

To estimate how well the two-equation turbulence model describes the actual flow structure over the entire flow field more experimental work is necessary.

Acknowledgement—Part of this work was sponsored by the Swedish Board for Technical Development. I wish to express thanks to professor N. Frössling for encouragement and good suggestions during the course of the work.

REFERENCES

1. J. Kestin, The effect of freestream turbulence on heat transfer rates, in *Advances in Heat Transfer*, Vol. 3, pp. 1–32. Academic Press, New York (1966).
2. B. Van der Hegge Zijnen, Heat transfer from horizontal cylinders to a turbulent air flow, *Appl. Sci. Res.* **7A**, 205–223 (1958).
3. B. Appelqvist, The influence of turbulence on the local heat transfer from a cylinder normal to an air stream, including further development of a method for local heat transfer measurements, Thesis for licenciatexamina, Department of Applied Thermo and Fluid Dynamics, Chalmers University of Technology, Göteborg (1965).
4. E. P. Dyban, E. Ya. Epick and L. G. Kozlova, Combined influence of turbulence intensity and longitudinal scale and air flow acceleration on heat transfer of circular cylinder, *Proc. Vth Int. Heat Transfer Conf.*, Tokyo (1974).
5. M. I. Boulos and D. C. T. Pei, Dynamics of heat transfer from cylinders in a turbulent air stream, *Int. J. Heat Mass Transfer* **17**, 767–783 (1974).
6. R. Liljevall, Increases in heat transfer by changing the turbulence structure of the flow field, STU-report 73-3647 (1975) (in Swedish).
7. R. Liljevall, to be published.
8. M. J. Lighthill, The response of laminar skin friction and heat transfer to fluctuations in the stream velocity, *Proc. R. Soc.* **A224** (1954).
9. C. C. Lin, Motion in the boundary layer with a rapidly oscillating external flow, *Ninth Int. Congress of Appl. Mech.*, University of Brussels, Belgium (1956).
10. M. B. Glauert, The laminar boundary layer on oscillating plates and cylinders, *J. Fluid Mech.* **1**, 97–110 (1956).
11. H. Ishigaki, Periodic boundary layer near a two-dimensional stagnation point, *J. Fluid Mech.* **43**, 477–486 (1970).
12. H. Ishigaki, Heat transfer in a periodic boundary layer near a two-dimensional stagnation point, *J. Fluid Mech.* **56**, 619–627 (1972).
13. S. P. Sutera, P. F. Maeder and J. Kestin, On the sensitivity of heat transfer in the stagnation point boundary layer to free stream vorticity, *J. Fluid Mech.* **16**, 497–520 (1963).
14. S. P. Sutera, Vorticity amplification in stagnation point flow and its effect on heat transfer, *J. Fluid Mech.* **21**, 513–534 (1965).
15. W. Z. Sadeh, S. P. Sutera and P. F. Maeder, Analysis of vorticity amplification in the flow approaching a two-dimensional stagnation point, *Z. angew. Math. Phys.* **21**, 699–716 (1970).
16. W. Z. Sadeh, S. P. Sutera and P. F. Maeder, An investigation of vorticity amplification in stagnation flow, *Z. angew. Math. Phys.* **21**, 717–742 (1970).
17. M. C. Smith and A. M. Kuethe, Effects of turbulence on laminar skin friction and heat transfer, *Physics Fluids* **9**, 2337–2344 (1966).
18. R. M. Traci and D. C. Wilcox, Analytical study of

freestream turbulence effects on stagnation point flow and heat transfer, *AIAA-Paper* 74–515 (1974).
19. R. M. Traci and D. C. Wilcox, Freestream turbulence effects on stagnation point heat transfer, *AIAA J.* **13**, 890–896 (1975).
20. J. C. R. Hunt, A theory of turbulent flow round two-dimensional bluff bodies, *J. Fluid Mech.* **61**, 625–706 (1973).
21. G. K. Batchelor and I. Proudman, The effect of rapid distortion of a fluid in turbulent motion, *Q. J. Mech. Appl. Math.* **7**, 83–103 (1954).
22. R. E. Britter, The distortion of turbulence by bluff bodies, Paper presented at the I.U.T.A.M. Congress at Delft (1976).
23. P. G. Saffman, A model for inhomogeneous turbulent flow, *Proc. R. Soc.* **A317**, 417–433 (1970).
24. D. C. Wilcox and I. E. Alber, A turbulence model for high speed flows, *Proc. 1972 Heat Transfer and Fluid Mechanics Institute*, June 14–16, 1972, Stanford Univ. Press (1972).
25. P. G. Saffman and D. C. Wilcox, Turbulence-model predictions for turbulent boundary layers, *AIAA J.* **12**, 541–546 (1974).
26. P. G. Saffman, Model equations for turbulent shear flows, *Stud. Appl. Math.* **LIII**, 17–34 (1974).
27. D. C. Wilcox, Turbulence-model transition predictions, *AIAA J.* **13**, 241–243 (1975).
28. W. P. Jones and B. E. Launder, The calculation of low-Reynolds number phenomena with a two-equation model of turbulence, *Int. J. Heat Mass Transfer* **16**, 1119–1130 (1973).
29. P. W. Bearman, Some measurements of the distortion of turbulence approaching a two-dimensional bluff body, *J. Fluid Mech.* **53**, 451–467 (1972).
30. J. Kestin, P. F. Maeder and H. Sogin, The influence of turbulence on the transfer of heat to cylinders near the stagnation point, *Z. Angew. Math. Phys.* **12**, 115–132 (1961).
31. G. M. Zapp, The effect of turbulence on local heat transfer coefficients around a cylinder normal to an air stream, Master's thesis, Oregon State University (1950).
32. W. H. Giedt, Investigation of variation of point unit heat transfer coefficient around a cylinder normal to an air stream, *Trans. ASME* **72**, 375–381 (1949).
33. H. Blasius, Grenzschichten in Flüssigkeiten mit kleiner Reibung, *Z. Math. Phys.* **56**, 1 (1908).
34. N. Frössling, Verdunstung, Wärmeübergang und Geschwindigkeitsverteilung bei zwei-dimensionaler und rotationssymmetrischer laminarer Grenzschicht-strömung, *Acta Univ. Lund.* **2**, 36 (1940).

ETUDE THEORIQUE DE L'INFLUENCE DE LA TURBULENCE DE L'ECOULEMENT LIBRE SUR LE FROTTEMENT ET LE TRANSFERT THERMIQUE A LA PAROI D'UN CORPS

Résumé—On présente une étude théorique de l'effet de la turbulence libre sur le frottement et le transfert thermique sur un cylindre circulaire en attaque transversale. Le champ d'écoulement est divisé en différentes régions. On utilise un modèle de turbulence à deux équations avec des transformations appropriées de coordonnées. Les calculs correspondent à des nombres de Reynolds entre 12 500 et 50 000, à des intensités de turbulence Tu_∞ variant de 1,25 à 6,1% et à des échelles de turbulence $\Lambda_{f\infty}/D$ entre 0,1 et 1,6. On détermine l'effet de l'intensité et de l'échelle de turbulence sur le frottement et sur le transfert thermique. Un bon accord est obtenu avec l'expérience.

EINE THEORETISCHE UNTERSUCHUNG ÜBER DEN EINFLUSS DER FREISTROMTURBULENZ AUF WANDREIBUNG UND WÄRMEÜBERGANG EINES STUMPFEN KÖRPERS

Zusammenfassung—Es wird über eine theoretische Untersuchung des Einflusses der Freistromturbulenz auf Wandreibung und Wärmeübergang an einem querangeströmten Kreiszylinder berichtet. Das Strömungsfeld wird in unterschiedliche Gebiete aufgeteilt. Ein Turbulenzmodell mit zwei Gleichungen und zweckmäßigen Koordinatentransformationen wird verwendet. Die Rechnungen werden für Reynolds-Zahlen im Bereich von 12 500–50 000, Turbulenzgrade im Bereich von $Tu_\infty = 1{,}25$–$6{,}1\%$ *sowie Turbulenzmaßstäbe im Bereich von* $\Lambda_{f\infty}/D = 0{,}1$–$1{,}6$ durchgeführt. Der Einfluß sowohl von Turbulenzgrad als auch von Turbulenzmaßstab auf Wandreibung und Wärmeübergang wurde gefunden und gute Übereinstimmung mit Experimenten erzielt.

ТЕОРЕТИЧЕСКОЕ ИССЛЕДОВАНИЕ ВЛИЯНИЯ ТУРБУЛЕНТНОСТИ СВОБОДНОГО ПОТОКА НА ПОВЕРХНОСТНОЕ ТРЕНИЕ И ТЕПЛОПЕРЕНОС ПЛОХООБТЕКАЕМОГО ТЕЛА

Аннотация — Представлено теоретическое исследование влияния турбулентности свободного потока на поверхностное трение и теплоперенос поперечно обтекаемого круглого цилиндра. Поле течения разделено на различные области. Для расчета характеристик турбулентности использована модель из двух уравнений ($k - \varepsilon$ модель). Расчеты выполнены для чисел Рейнольдса в диапазоне 12 500–50 000, интенсивности турбулентности, Tu_∞, в пределах 1,25–6,1% и масштаба турбулентности в диапазоне $\Lambda_{f\infty}/D = 0{,}1$–$1{,}6$. Обнаружено влияние на поверхностное трение и теплоперенос как интенсивности, так и масштаба турбулентности. Получено хорошее согласие с экспериментом.